

## Time-Resolved X-Ray Scattering Study of Ordering and Coarsening in $\text{Cu}_3\text{Au}$

S. E. Nagler, R. F. Shannon, Jr., C. R. Harkless, and M. A. Singh

*Department of Physics, University of Florida, Gainesville, Florida 32611*

and

R. M. Nicklow

*Oak Ridge National Laboratory, Oak Ridge, Tennessee 37831*

(Received 10 March 1988)

The kinetics of ordering and coarsening in single-crystal  $\text{Cu}_3\text{Au}$  are studied by use of time-resolved x-ray scattering. After a quenching from high temperatures to fixed temperatures below the order-disorder temperature, three regimes are apparent: nucleation, ordering, and coarsening. The superlattice peaks are anisotropic, reflecting the domain structure. The line shape of the scattering function changes with time during the crossover from the ordering to the coarsening regime. The late-stage coarsening is consistent with curvature-driven growth.

PACS numbers: 61.50.Ks, 64.60.Cn, 64.60.My, 82.20.Mj

The nonequilibrium kinetics of first-order phase transitions is one of the most fascinating problems in statistical physics.<sup>1</sup> Evidence<sup>1-5</sup> from theory, computer simulations, and experiments indicates that universal laws exist for the late-time development of long-range order in a system approaching equilibrium after a quench. The criteria for different universality classes remains an open question, but must at least include whether the order parameter is conserved or nonconserved, and the degeneracy,  $p$ , of the ordered ground state.<sup>6</sup>

Binary alloys are convenient model systems for investigating kinetic phenomena. The conserved-order-parameter (COP) process of phase separation has been extensively studied experimentally.<sup>1,2,7,8</sup> Surprisingly, there has been far less investigation of the approach to equilibrium in order-disorder transitions, in which the order parameter is nonconserved (NCOP).<sup>9-12</sup> In this Letter we report a time-resolved x-ray scattering study of the approach to equilibrium in  $\text{Cu}_3\text{Au}$ . The results confirm that three distinct physical regimes can be distinguished: nucleation, ordering, and coarsening.<sup>13</sup> The two types of domain walls<sup>14</sup> that form in  $\text{Cu}_3\text{Au}$  give rise to anisotropic scattering at reciprocal-space superlattice points characterizing the order.<sup>15</sup> In addition, the late-time scaling limit can be identified via the evolution of the scattering line shapes.

The situation is depicted schematically in Fig. 1. Initially the alloy is annealed at high temperatures in the disordered state, and at time  $t=0$  it is rapidly quenched to a fixed temperature below the ordering temperature,  $T_c$ . After the quench, a nonzero incubation time may elapse before the onset of critical nucleation. Droplets of the ordered phase then appear, embedded in a matrix of disordered phase [Fig. 1(a)]. The individual droplets may be in any of the  $p$ -allowed ground states. As time passes, the isolated droplets grow in size; this process may be termed ordering. Eventually the domain meet

[Fig. 1(b)], and the system is composed of domains in different ground states separated by domain walls. At this point the coarsening process begins and the average size of the domains continues to grow [Figs. 1(b) and 1(c)].

At late times in the coarsening regime the system can be characterized by a single length scale,  $L(t)$ , the average size of an ordered domain at time  $t$ .<sup>1</sup> The system is then self-similar under a rescaling of both space and time. The domain size grows with a characteristic power law,

$$L(t) \sim t^a. \quad (1)$$

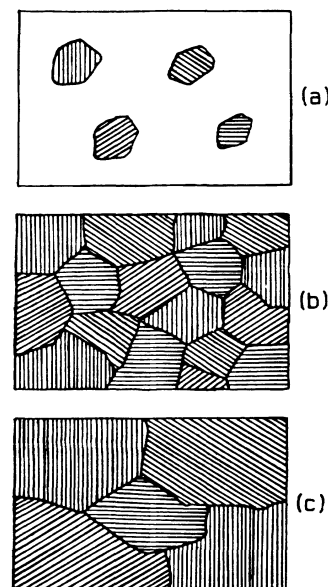


FIG. 1. Ordering and coarsening after a quench: (a) ordering shortly after the onset of critical nucleation; (b) early stages of domain coarsening; (c) late-stage coarsening.

For curvature-driven growth, one expects  $a = \frac{1}{2}$ ; this is known to be correct for a NCOP system with  $p=2$  and no random impurities.<sup>16,17</sup> The structure factor for the order parameter also exhibits scaling<sup>1</sup> of the form

$$S(\mathbf{Q}, t) = [L(t)]^d \tilde{S}_e(qL(t)), \quad (2)$$

where  $\mathbf{q} = \mathbf{Q} - \mathbf{G}$ ,  $\mathbf{G}$  is the ordering wave vector,  $d$  is the spatial dimensionality, and  $\hat{\mathbf{e}} = \mathbf{q}/q$ . The scaling function  $\tilde{S}$  is in general anisotropic, and reflects the structure of the domains and the form of the domain walls.<sup>3</sup>

The  $\text{Cu}_3\text{Au}$  system has been widely studied and is a classic example of the order-disorder transition.<sup>15</sup> The solid solution forms a fcc crystal and below  $T_c \approx 390^\circ\text{C}$  orders in the  $L1_2$  structure (Au on the corners, Cu on the face centers) with ground-state degeneracy  $p=4$ . Using time-resolved x-ray techniques, Noda, Nishimura, and Takeuchi<sup>9</sup> measured radial scans of the [110] superlattice in  $\text{Cu}_3\text{Au}$  after quenching from just above  $T_c$ . Assuming isotropic scattering profiles, they found evidence for scaling of  $S(\mathbf{Q}, t)$ , a Lorentzian-squared line shape, and curvature-driven growth.

In fact, it is well known<sup>15</sup> that the superlattice profiles in  $\text{Cu}_3\text{Au}$  are not isotropic. Low-energy, half-diagonal glide domain walls (type-1 walls)<sup>14</sup> form very easily and result in a characteristic disk-shaped profile. Higher-energy type-2 walls, consisting of adjacent 100% Cu or 50% Cu layers, result in a nonzero thickness of the disk. Measurements of the full anisotropic profile probes domain growth associated with the motion of both types of walls. The present results establish the validity of scaling in an anisotropic system. The resolution is improved by a factor of 2 over previous measurements, and it is found that different physical regimes are marked by changes in the observed line shape. Also, it is clearly seen that scaling is valid only in the coarsening regime, not during the ordering process.

The  $\text{Cu}_3\text{Au}$  single crystal was cut to expose a  $[h00]$  face which was prepared by polishing and etching with nitric acid followed by annealing for 12 h at  $700^\circ\text{C}$  under an Ar atmosphere. The order-disorder transition temperature was found to be  $T_c = 385.3^\circ\text{C}$ .

In a typical time-resolved measurement the sample was annealed at high temperatures for 5–12 h, and then cooled to a temperature of  $\sim 405^\circ\text{C}$ . The sample was then quenched rapidly to a final temperature  $T_f$ . Typical quenching times of 1 min were required to achieve a stable final temperature, controlled to  $\pm 0.5^\circ\text{C}$  over many days.

After quenching, the [100] superlattice peak was studied in detail. To within experimental resolution the scattering was a circular disk with an  $(h, 0, 0)$  axis of symmetry. Transverse scans through the disk along the  $(0, k, 0)$  direction were done with the use of a rotating-anode point source of  $\text{Cu-K}\alpha$  radiation and a flat pyrolytic graphite [002] monochromator and analyzer. Radial scans were done with a line source, monochromator, and

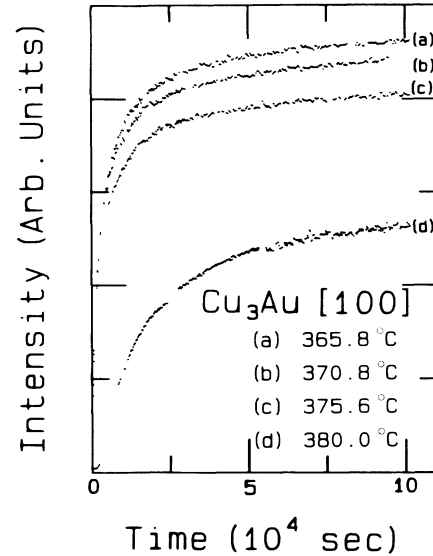


FIG. 2. Integrated intensity vs time after quenching. The data are normalized to the same monitor count of incident photons and corrected for detector dead time.

a linear position-sensitive detector. For each of these configurations, the instrumental resolution was  $0.003 \text{ \AA}^{-1}$  HWHM in the direction scanned.

The integrated intensity versus time after quenching is displayed in Fig. 2 for some representative temperatures. The data shown were obtained from transverse scans. The results for all temperatures show the same general features. Immediately after some quenches there is a delay during which no additional intensity is observed. For shallow quenches the delay is appreciable and is clearly visible in the  $380.0^\circ\text{C}$  data of Fig. 2. Following the delay a rapid growth in the intensity is observed corresponding to a linear rise with time. At late times the intensity saturates at a value  $I_\infty(T)$ . Plotting  $I/I_\infty$  vs  $t/\tau$ , where  $\tau$  is the time for the intensity to reach  $I_\infty/2$ , reveals that the scaled data for different temperatures fall on a universal curve.<sup>9</sup>

The delay at early times can be associated with an incubation time for nucleation. This behavior has been observed clearly in single grains of  $\text{Mg}_3\text{In}$  by Konishi and Noda.<sup>18</sup> The time depends on sample history and varies among individual grains. The result in polycrystalline or mosaic samples is a smearing of the curve.

The rapid rise in intensity followed by saturation is consistent with observations in other systems, such as graphite intercalates.<sup>19</sup> The origin of this feature is illuminated by examination of the shape of the scattering profile. Figure 3 shows a transverse scan through the [100] peak at times 450 and 2600 sec after a quench to  $365.8^\circ\text{C}$ . The general features observed are the same at all quench depths. The profiles obtained during the early stages of the fast rise in intensity are well described by Gaussian (GS) line shapes. At late times the line shape

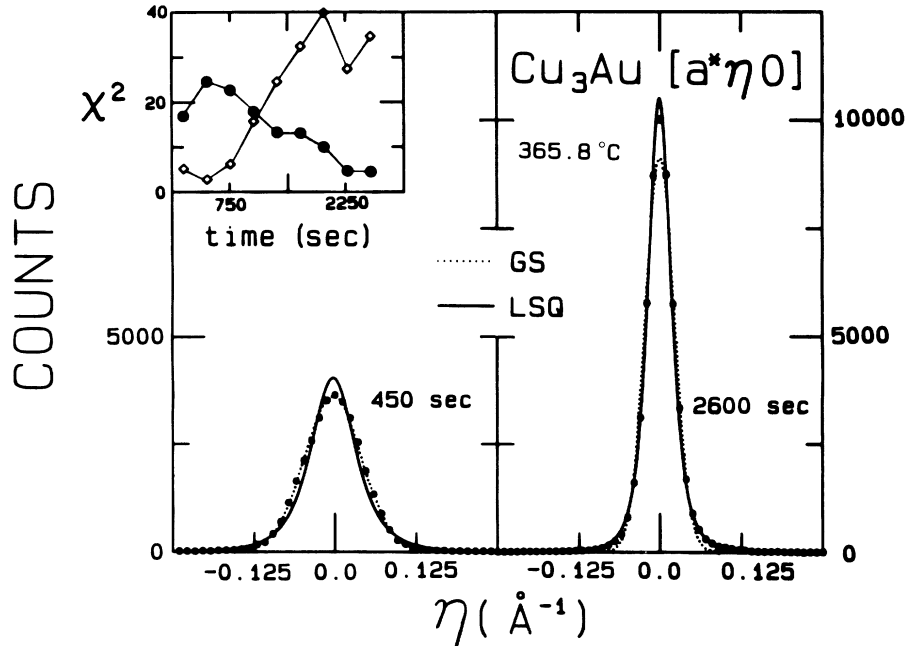


FIG. 3. Evolution of the line shape after a quench. The transverse scans are through the [100] superlattice peak with  $a^* = 1.666 \text{ \AA}^{-1}$ . The solid and dotted lines are the best least-squares fits with the model line shapes discussed in the text. The FWHM of the instrumental resolution is equal to the width of the tic marks on the  $\eta$  axis. Inset:  $\chi^2$  of the fit vs time after the quench for the GS (diamonds) and LSQ (circles) line shapes.

crosses over to a Lorentzian-squared (LSQ) form. A simple Lorentzian line shape cannot describe the data at any time. The GS line shape is associated with finite-size broadening and is found in superlattice peaks arising from isolated ordered clusters embedded in a disordered matrix. It is therefore characteristic of the ordering process. The LSQ shape, which is characteristic of the coarsening process, results from a random distribution of ordered domains that are separated by sharp walls.<sup>20</sup> Various theoretical predictions show<sup>5,21</sup> that for coarsening in three dimensions the tails of  $S(\mathbf{q}, t)$  should decay as  $q^{-4}$ , consistent with the LSQ. As shown by the inset to Fig. 3, the scattering line shapes exhibit a crossover from GS to LSQ behavior with time. The LSQ line shape is clearly a signature of the late-time scaling regime.

The width of the LSQ profile is a measure of  $L^{-1}(t)$ . The scattering profiles were fitted by a function of the form  $A/\{1 + \frac{1}{2} [(Q - G)/\Gamma]^2\}^2$ . The observed scattering is a convolution of the intrinsic line shape with an effective resolution function containing the instrumental broadening as well as independently measured corrections for mosaic spread and strain. Figure 4 shows plots of  $\log_{10}(\Gamma)$  vs  $\log_{10}(t)$  for two representative temperatures. Data are presented for both the broad transverse scan and narrow radial scans. The intrinsic widths are much broader than the resolution limit except for the very-late-time data in the radial scans. The solid lines represent power-law fits [Eq. (1)] to the late-time data. It is apparent that the scaling regime is approached more

slowly for shallower quench depths.<sup>9</sup> The results for the growth exponent  $a$ , summarized in Table I, are consistent with curvature-driven growth ( $a = \frac{1}{2}$ ) over most

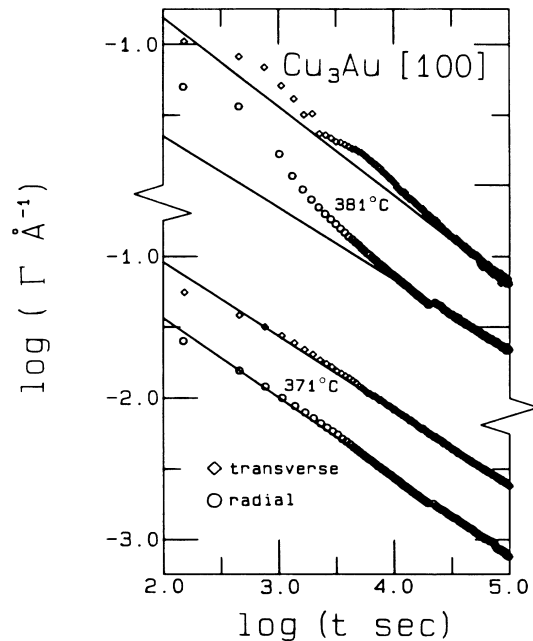


FIG. 4. Linewidth vs time after the quench. Solid lines are typical power-law fits as discussed in the text. The data shown have been linearly corrected for extra broadening arising from the effective resolution.

TABLE I. Fitted growth exponents ( $a$ ) for the [100] superlattice peak.

$T$	Transverse	Radial
365.8 °C	0.52	0.56
370.8 °C	0.52	0.56
375.6 °C	0.52	0.59
380.0 °C	0.59	...
382.0 °C	...	0.55

of the range studied. The resolution correction is the principal source of uncertainty in the determination of  $a$ . We estimate the accuracy of the exponents in Table I to be (10–20)%. Within these limits, it is seen that the radial and transverse widths exhibit the same exponents. This result is independent of temperature, and was adumbrated by previous measurements on textured thin films of  $\text{Cu}_3\text{Au}$ .<sup>22</sup> It is a strong confirmation of anisotropic scaling,<sup>3</sup> and implies that the curvature-driven growth mechanism applies to different types of walls. At very late times the transverse-scan data show possible hints of slower growth. This may arise from the presence of impurities or slightly incorrect stoichiometry in the layer being probed, either of which could lead to a  $\log(t)$  growth law.<sup>23–26</sup>

In summary, we conclude that the kinetics of the order-disorder phase transition in  $\text{Cu}_3\text{Au}$  displays regimes of nucleation, ordering, and coarsening. The ordering and coarsening regimes may be distinguished experimentally by the line shape of the superlattice peaks.  $S(\mathbf{q}, t)$  is anisotropic, reflecting the structure of the underlying domains. The late stage of coarsening is consistent with a curvature-driven growth law for both types of domain walls. A full, detailed account of this work will be published elsewhere.

We are grateful to D. N. Zehner and G. W. Ownby for their aid in the preparation of the sample. It is a pleasure to acknowledge useful discussions with J. Gunton, P. Kumar, G. Mazenko, S. Moss, Y. Noda, D. Srolovitz, and N. Sullivan. Excellent technical assistance was provided by W. Ruby. This research was supported by the U.S. Department of Energy (Office of Basic Energy Sciences) under Grant No. DE-FG05-86ER45280. The work of one of us (S.E.N.) was supported by the National Science Foundation (DMR-8553282). Oak Ridge National Laboratory is operated by Martin

Marietta Energy Systems Inc. for the U.S. Department of Energy under Contract No. De-AC05-85OR21400.

<sup>1</sup>For extensive review, see J. D. Gunton, M. San Miguel, and P. S. Sahni, in *Phase Transitions and Critical Phenomena*, edited by C. Domb and J. Lebowitz (Academic, New York, 1983), Vol. 8.

<sup>2</sup>G. F. Mazenko, O. T. Valls, and F. C. Zhang, *Phys. Rev. B* **31**, 4453 (1985).

<sup>3</sup>G. F. Mazenko and O. T. Valls, *Phys. Rev. B* **30**, 6732 (1984).

<sup>4</sup>A. Milchev, K. Binder, and D. W. Heerman, *Z. Phys.* **B63**, 521 (1986).

<sup>5</sup>G. Mazenko, O. T. Valls, and M. Zannetti, to be published.

<sup>6</sup>K. Binder, in *Statistical Physics*, edited by H. E. Stanley (North-Holland, New York, 1986).

<sup>7</sup>M. Hennion, D. Ronzaud, and P. Guyot, *Acta Metall.* **30**, 599 (1982).

<sup>8</sup>S. Katano and M. Iizumi, *Phys. Rev. Lett.* **52**, 835 (1984).

<sup>9</sup>Y. Noda, S. Nishihara, and Y. Yamada, *J. Phys. Soc. Jpn.* **53**, 4241 (1984).

<sup>10</sup>T. Hashimoto, K. Nishimura, and Y. Takeuchi, *J. Phys. Soc. Jpn.* **45**, 1127 (1978).

<sup>11</sup>N. Wakabayashi, *Phys. Rev. B* **33**, 6441 (1986).

<sup>12</sup>H. Chen and J. B. Cohen, *J. Phys. (Paris)* **C7**, 314 (1977).

<sup>13</sup>These regimes are discussed by F. P. Burns and S. L. Quimby, *Phys. Rev.* **97**, 1567 (1955).

<sup>14</sup>R. Kikuchi and J. W. Cahn, *Acta Metall.* **27**, 1085 (1979).

<sup>15</sup>For example, see B. Warren, *X-Ray Diffraction* (Addison-Wesley, Reading, MA, 1969).

<sup>16</sup>I. M. Lifshitz, *Zh. Eksp. Teor. Fiz.* **42**, 1354 (1962) [*Sov. Phys. JETP* **15**, 939 (1962)].

<sup>17</sup>S. M. Allen and J. W. Cahn, *Acta Metall.* **27**, 1085 (1979).

<sup>18</sup>H. Konishi and Y. Noda, to be published.

<sup>19</sup>P. Hernandez *et al.*, *Phys. Rev. Lett.* **59**, 1220 (1987).

<sup>20</sup>P. Debye, H. R. Anderson, Jr., and H. Brumberger, *J. Appl. Phys.* **28**, 679 (1957).

<sup>21</sup>T. Ohta, D. Jasnow, and K. Kawasaki, *Phys. Rev. Lett.* **49**, 1223 (1982).

<sup>22</sup>S. E. Nagler, R. F. Shannon, Jr., and C. R. Harkless, in "Dynamics of Ordering Processes," edited by S. Komura (Plenum, New York, to be published).

<sup>23</sup>D. J. Srolovitz and G. M. Hassold, *Phys. Rev. B* **35**, 6902 (1987).

<sup>24</sup>G. S. Grest and D. J. Srolovitz, *Phys. Rev. B* **32**, 3014 (1985).

<sup>25</sup>D. Chowdury, M. Grant, and J. D. Gunton, *Phys. Rev. B* **35**, 6792 (1987).

<sup>26</sup>R. F. Shannon, Jr., C. R. Harkless, and S. E. Nagler, to be published.